AD-A018 619

GALLIUM ARSENIDE PHOTOCATHODE DEVELOPMENT

Terry Roach, et al

EPSCO Laboratories

Prepared for:

Rome Air Development Center
Defense Advanced Research Projects Agency

October 1975

RADC-TR-75-254
Final Technical Report
October 1975

GALLIUM ARSENIDE PHOTOCATHODE DEVELOPMENT

EPSCO Laboratories

Sponsored by
Defense Advanced Research Projects Agency
ARPA Order No. 1965

Rome Air Development Center
Air Force Systems Command
Griffiss Air Force Base, New York 13441

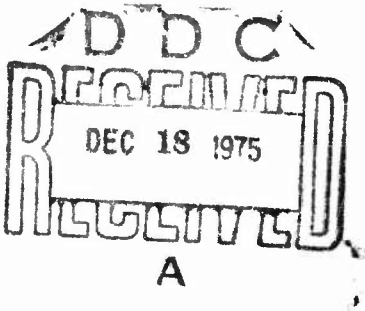

GALLIUM ARSENIDE PHOTOCATHODE DEVELOPMENT

T. Roach
J. Bianca

Contractor: EPSCO Laboratories
Contract Number: F08606-73-C-0028
Effective Date of Contract: 3 January 1973
Contract Expiration Date: 15 August 1975
Amount of Contract: $5,056,595.00
Program Code Number: 5E20
Period of work covered: 6 Jun 73 - 31 Dec 74

Principal Investigator: Terry Roach
203 327-2000

Project Engineer: Thomas G. Pitts
315 330-3145

This research was supported by the Defense Advanced Research Projects Agency of the Department of Defense and was monitored by Thomas G. Pitts, RADC (OCSE), Griffiss Air Force Base, New York 13441.

UNCLASSIFIED

SECURITY CLASSIFICATION OF THIS PAGE (When Data Entered)

REPORT DOCUMENTATION PAGE		READ INSTRUCTIONS BEFORE COMPLETING FORM
1. REPORT NUMBER RADC-TR-75-254	2. GOVT ACCESSION NO.	3. RECIPIENT'S CATALOG NUMBER
4. TITLE (and Subtitle) GALLIUM ARSENIDE PHOTOCATHODE DEVELOPMENT		5. TYPE OF REPORT & PERIOD COVERED Final Technical Report 6 Jun 73 - 31 Dec 74
		6. PERFORMING ORG. REPORT NUMBER N/A
7. AUTHOR(s) T. Roach J. Bianca		8. CONTRACT OR GRANT NUMBER(s) F08606-73-C-0028
9. PERFORMING ORGANIZATION NAME AND ADDRESS EPSCO Laboratories 227 High Ridge Road Stamford CT 06905		10. PROGRAM ELEMENT, PROJECT, TASK AREA & WORK UNIT NUMBERS 62301E 19650101
11. CONTROLLING OFFICE NAME AND ADDRESS Defense Advanced Research Projects Agency 1400 Wilson Blvd Arlington VA 22209		12. REPORT DATE October 1975 13. NUMBER OF PAGES 54
14. MONITORING AGENCY NAME & ADDRESS(if different from Controlling Office) Rome Air Development Center (OCSE) Griffiss AFB NY 13441		15. SECURITY CLASS. (of this report) UNCLASSIFIED 15a. DECLASSIFICATION/DOWNGRADING SCHEDULE N/A

16. DISTRIBUTION STATEMENT (of this Report)

Approved for public release; distribution unlimited.

17. DISTRIBUTION STATEMENT (of the abstract entered in Block 20, if different from Report)

Same

18. SUPPLEMENTARY NOTES

RADC Project Engineer:
Thomas G. Pitts/OCSE

19. KEY WORDS (Continue on reverse side if necessary and identify by block number)

Photocathode
Terniary Compounds
Quantum Efficiency

20. ABSTRACT (Continue on reverse side if necessary and identify by block number)

This report presents the final results of a task to investigate III-V photoemitter technology for application to image sensors. Investigations of crystal surface preparation, the physics of GaAs photoemission, photocathode processing techniques, GaAs photocathode characteristics and reprocessing techniques have been completed. Emphasis was placed on the development of a transmissive GaAs photocathode with sensitivity, uniformity, size and life suitable for high resolution low light level imaging applications.

DD FORM 1 JAN 73 1473 EDITION OF 1 NOV 65 IS OBSOLETE

UNCLASSIFIED

SECURITY CLASSIFICATION OF THIS PAGE (When Data Entered)

ABSTRACT

This report details the results of an experimental program to develop III-V photoemitter technology for application to a Teal Blue electronic camera.

The procedures involving in-vacuo crystal surface preparation and activation are discussed.

A description of a revised understanding of the physics of GaAs photoemission is included.

The equipment required for GaAs photocathode processing and transfer is discussed.

A significant discovery has been made whereby an activated GaAs crystal can be exposed to atmosphere and subsequently reprocessed to near-original sensitivity.

TABLE OF CONTENTS

LIST OF ILLUSTRATIONS

TITLE

LIST OF TABLES

SECTION 1

1.0 OBJECTIVES

The major thrust of the program effort applied existing III-V photocathode technology to the specific application of developing a processing method and physical structure for a transmissive photocathode with performance characteristics (sensitivity, uniformity, size and life) suitable for future project use.

The goals were stable operation of a Gallium Arsenide photocathode, transferred into a benign environment, with a spectral sensitivity in excess of 40 ma/W over the range of 550 to 850 nanometers and quantum efficiency of 8% or more at 700 nm for a 1 cm by 1 cm emitting area.

The development of the high quantum efficiency photocathode followed a logical sequence:

1. "In vacuo" crystal surface cleaning and lattice damage reduction, principally utilizing thermal techniques,

2. Cathode activation to a stable emissive condition

3. Extension of the crystal preparation and cathode activation techniques to obtain emission uniformity over the desired cathode area,

4. An apparatus suitable for cathode activation and subsequent cathode transfer into an adjacent benign environment test envelope was constructed,

5. Stability mechanisms and requirements for extended life in the benign environment were investigated,

6. The technology accumulated in the foregoing series of experiments was applied to the activation of semi-transparent (transmissive) GaAs and GaAs on GaP crystals, and

7. As originally planned, the program included the development of a larger format (2 cm x 2 cm) GaAs photocathode based on a detailed study of materials parameters and the application of crystal preparation and activation techniques developed for the 1 cm x 1 cm GaAs photocathode.

   The use of ternary III-V compounds such as GaInAs to obtain 1.06 um response was to be investigated.

A restructuring of the overall program deleted the tasks in Group 7 prior to any significant expenditure.

SECTION 2

CRYSTAL ACTIVATIONS

2.1 CRYSTAL SURFACE PREPARATION IN VACUO

It is absolutely necessary that the crystal surface that will be emitting the photoelectrons into the vacuum be atomically clean and relatively free of crystalline defects.

The accepted method of cleaning the crystal in vacuo is by heating it to a sufficient temperature to desorb the surface contaminants, which also provides an annealing action which reduces the residual crystal lattice damage.

However, the temperature required to provide adequate surface conditioning is very close to that which will cause irreversible damage to the bulk crystal. Arsenic, which has a higher vapor pressure than gallium, is desorbed first, leaving a surplus of metallic gallium which, in extreme cases, is visible in globular form on the crystal surface. Since a certain threshold gallium-rich imbalance of the crystal surface must be reached before good emission properties can be obtained, the thermal treatment of the crystal must be rigidly controlled to provide an atomically clean surface with minimum crystal lattice damage and yet preserve the desired surface stoichiometry.

The time period between the substrate cleaning and the cathode activation must be significantly less than that required for redeposition of the contaminating gases from the ambient vacuum. This requires system pressures less than 10^{-10} torr and a vacuum system design that permits rapid cooling of the crystal following the heat treatment.

2.2 CESIUM-OXYGEN SURFACE ACTIVATION

The photoelectrons generated within the GaAs crystal must be emitted into the device vacuum to be useful. This requires that the electrons overcome the potential barrier (work function) existing at the crystal-vacuum interface. The purpose of the surface activation is to lower the surface work function, considerably increasing the probability of electron emission.

To provide the optimum emission characteristic, a controlled amount of cesium and oxygen is deposited on the atomically clean GaAs surface. The stoichiometry of this surface treatment is controlled during the activation process to provide the desired emission characteristics.

2.3 SEQUENCE OF EXPERIMENTS

A total of 491 activations on 40 individual GaAs crystals, both opaque and semitransparent, have been carried out during this program as shown in Table 1. A natural evolution of experiments was followed and will be explained here.

TABLE I (1 of 4)

SUMMARY OF GaAs SURFACE ACTIVATIONS

Sample No.	Crystal Type	Total No. of Activatione	Activation No. of Peak Sensitivity	Radiant Sensitivity @ 700 nm	Quantum Efficiency @ 700 nm	Luminoue Sensitivity	System Type, Stability and Other Comments
1	Used to correlate eubetrate thermocouple readinge and infrared radiation pyrometer						Demountable bell jar
2	MC7 5-7 x $10^{18}cm^{-3}$ Batch #1	6	6	100 mA/wett	17.7%		Demountable bell jar Previously ectivated cesium channel
3	Same	5	2	36 mA/watt	6.4%		Demountable bell jar Freeh cesium channel
4	Leak in electrical feedthrough - Rework!						Demountable bell jar cesium ampoule
5	Same	7	7	44 mA/watt	7.7%	258 µA/lumen	Demountable bell jar Change to Cs channel after 2 runs; O_2 leak modified.
6	Same	8	7	53 mA/watt	9.4%	410 µA/lumen	Demountable bell jar Old channel.
7	MC7 5-7 x $10^{18}cm^{-3}$ except Batch #2	11	8	61 mA/watt	10.8%	506 µA/lumen	Demountable bell jer New channel.
8	Same	7	4	54 mA/watt	9.6%	429 µA/lumen	Demountable bell jer Old channel.
9	New collector errangement evidently ineffectuel - no eppreciable sensitivity						Demountable bell jar New chennel Modify S.S. holder.
10	Same	13	5	80 mA/watt	13.2%		Demountable bell jer Elemental Cs source port
11	High preeeure Ce eource opened - change eource						Demountable bell jer Redesign Cs spout (beam off center)
12	Same	13	8	57 mA/watt	10.1%	535 µA/luman	Demountable bell jar Elemental Cs source; tantalum spray spout
13	Same	15	13	153 mA/watt	27.1%	1351 µA/lumen	Demountable bell jer Elemental Cs source

TABLE I (2 of 4)
SUMMARY OF GaAs SURFACE ACTIVATIONS

Sample No.	Crystal Type	Total No. of Activations	Activation No. of Peak Sensitivity	Radiant Sensitivity @ 700 nm	Quantum Efficiency @ 700 nm	Luminous Sensitivity	System Type, Stability and Other Comments
14	Same	4	2	105 mA/watt	18.6%		Demountable bell jar crystals etched in 5:1:1 (H_2SO_4:H_2O_2:H_2O) solution (10 sec.)
15	Same	No appreciable sensitivity - Samples #14 & #15					Demountable bell jar Etched prior to vacuum entry
16	Same	11	2	146 mA/watt	26%	1320 µA/lumen	Demountable bell jar Elemental Cs source
17	Same	21	15	178 mA/watt	32%	1670 µA/lumen	Demountable bell jar 60% of peak sensitivity after 18 hours.
18	5-7 x $10^{18}cm^{-3}$ zinc	14	12	151 mA/watt	27%	1328 µA/lumen	Demountable bell jar, 62% of peak sensitivity after 17 hrs. Reevacuated and activated in transfer chamber.
	MC7 Batch #2	15	10	124 mA/watt	22%	1075 µA/lumen	
19	Same	18	16	145 mA/watt	26%	1287 µA/lumen	Demountable bell jar
20	Same	14	10	142 mA/watt	25%	1283 µA/lumen	Demountable bell jar
21	1 x $10^{19}cm^{-3}$ zinc MC7	14	9	74 mA/watt	13%	605 µA/lumen	Demountable bell jar
22	Same	9	8	86 mA/watt	15%	710 µA/lumen	Demountable bell jar
23	Same	8	6	90 mA/watt	16%	750 µA/lumen	Demountable bell jar
24	6-8 x $10^{18}cm^{-3}$ zinc MC19A	9	7	40 mA/watt	7%		Demountable bell jar, 1 µm GaAs on GaP window.
25	Same	18	17	53 mA/watt	9%		Demountable bell jar 1 µm GaAs on GaP window.

TABLE I (3 of 4)

SUMMARY OF GaAs SURFACE ACTIVATIONS

Sample No.	Crystal Type	Totel No. of Activations	Activation No. of Peak Sensitivity	Radiant Sensitivity @ 700 nm	Quantum Efficiency @ 700 nm	Luminous Sensitivity	System Type, Stability and Other Comments
26	5-7 x $10^{13}cm^{-3}$ zinc MC7 Batch #2	First of Tranefer Chamber Experiments No appreciable sensitivity					
27	Same	14	2	84 mA/watt	15%	785 µA/lumen	Transfer chamber, 100% of peak sensitivity after 15 hrs.
28	5-7 x $10^{18}cm^{-3}$ zinc MC7 Batch #2	10	8	35 mA/watt	6%		Transfer Chamber
29	5-7 x $10^{18}cm^{-3}$ zinc MC7 Batch #2	11	8	80 mA/watt	14%		Transfer Chamber, Cesium Channel used for passivation of chamber
30	5-7 x $10^{18}cm^{-3}$ zinc MC7 #1-553	12	5	81 mA/watt	14%	684 µA/lumen	Transfer chamber
31	Same	17	14	65 mA/watt	11%		Demountable bell jar
		12	10	84 mA/watt	15%	685 µA/lumen	
32	Same	9	5	61 mA/watt	11%	506 µA/lumen	Transfer chamber
33	2-4 x $10^{18}cm^{-3}$ zinc MC7 #1-595	13	9	65 mA/watt	12%		Transfer chamber
34 (Tranefer #1)	6.2 x $10^{18}cm^{-3}$ zinc MC7, one replecement crystal for test	9	4	115 mA/watt	20%		Transfer chamber Non-transferrable.
		17	Transfer Sensitivity	98 mA/watt	17%		Transfer apparatus installed. Transfer aborted - malfunction in mechanical pick-up.
		7	Transfer Sensitivity	90 mA/watt	16%		Let to air, realign pick-up assembly & reevacuate, transfer aborted-malfunctions

TABLE I (4 of 4)

SUMMARY OF GaAs SURFACE ACTIVATIONS

Sample No.	Crystal Type	Total No. of Activations	Activation No. of Peak Sensitivity	Radiant Sensitivity @ 700 nm	Quantum Efficiency @ 700 nm	Luminous Sensitivity	System Type, Stability and Other Comments
Self-Supporting #1	5-7 x $10^{18}cm^{-3}$ zinc Thin film on sapphire	19	17	66 mA/watt	12%	557 μA/lumen	Demountable bell jar
Transfer #2	5-7 x $10^{18}cm^{-3}$ zinc MC7 #1-673	Presently in vacuo					
Transfer #3	Sample #17	15	Post Transfer Sensitivity	100 mA/watt	18%	911 μA/lumen	Reevacuated sample #17
Transfer #4	6.2 x $10^{18}cm^{-3}$ zinc MC & replacement	29	Post Transfer Sensitivity	68 mA/watt	12%		Transfer chamber
Self-Supporting #2	5-7 x $10^{18}cm^{-3}$ zinc thin film on sapphire	No results: Surface layer developed before any appreciable sensitivity could be attained.					
35	6.2 x $10^{18}cm^{-3}$ zinc MC7 replacement	No results: High amount of dissociation					Demountable bell jar
36	MC19A GaAs/GaP	Surface layer developed		26 mA/watt			Transfer chamber

NOTE: All measurements taken in the reflective mode unless otherwise stated

The first experiment undertaken was to obtain a reproducible method of crystal temperature monitoring during heat cleaning. A chromel-alumel thermocouple was placed on the surface of Sample #1, (see Table 1) and its readings were correlated to a remote infrared radiation pyrometer (IRP). Although the IRP did not read the actual surface temperature of the crystal, it could consistently be related to the temperature of incipient dissociation needed to provide adequate surface cleaning. Because of this reproducibility the IRP was chosen as the tool to monitor temperature during heat cleaning.

Next in line was to obtain a heat cleaning procedure and photo-activation technique using cesium and oxygen that yielded optimum photoemission in the reflective mode. Individual experiments using Samples #2 - #20 were carried out in the demountable belljar. The crystals used for this consisted of a <110> 10 micron thick epitaxial layer of GaAs doped with zinc to 5-7 x 10^{18} cm^{-3}, vapor-deposited on a GaAs substrate.

In order to obtain optimum photoemission, certain system changes were inevitable. A time lag in the admission of oxygen appeared to be detrimental during activation and therefore warranted a faster responding oxygen admission system. Direct coupling of the silver tube (which when heated admits oxygen) to the vacuum chamber was incorporated and eliminated the time lag problem.

High background pressure and ion bombardment during activation was the next problem encountered. This was found to be an inherent fault with the particular type of cesium generator used, so a new cesium source was pursued. An ampoule filled with cesium distilled from a channel was tried, this proved to be uncontrollable, however. An elemental cesium source port was then built as used by W. Klein from NVL[1]. This proved to be successful after small directional and uniformity of admission problems were curtailed by redesigning the cesium input spout to incorporate a tantalum diffuser hat.

With these problems rectified, an optimum activation procedure was defined as follows: The crystal was heat cleaned at a temperature just below that of dissociation. While monitoring photoemission, the sample was cesiated as it cooled to peak photoemission and then driven down to 30% of its peak. Oxygen was then admitted until photoemission peaked and fell off to 10%. This procedure was repeated until peak photoemission was achieved. A lower-temperature heat treatment immediately followed and the above activation procedure was repeated.

Using this procedure, luminous sensitivities as high as 1350 μamperes/lumen with radiant sensitivities of 150 milliamps/watt at 700 nm were attained. Reproducibility of comparable sensitivities allowed this phase of experimentation to be curtailed. It should be noted that some stability was recorded on Samples #17 and #18 in the area of 60% of the peak sensitivity at 700 nm after 18 hours (in the chamber environment).

---

1 Wolfgang Klein, Rev. Sci. Instrum., 42, July 1971.

The next series of experiments was directed towards the determination of the optimum doping density for the final transmissive photocathodes. Samples #21 - #23 and #33 were used in this effort with doping densities of 1 x 10^{19} cm^{-3} zinc and 2-4 x 10^{18} cm^{-3} zinc respectively. The resultant performance of the crystals are analyzed and discussed in the section on GaAs Crystal Evaluation. It was concluded from these results that the original doping density of 5-7 x 10^{18} cm^{-3} zinc, tried in the early experiments, represented the optimum for the transmissive photocathode.

The performance of a 1-micron thick GaAs epitaxial layer on a GaP substrate was then investigated, since this crystal could be used in the transmissive mode. These samples (Samples #24 and #25) were activated in the demountable belljar allowing only reflective mode measurements. Poor results (only 53 mA/watt at 700 nm), however, discouraged further pursuit.

The next task undertaken was the design, fabrication and implementation of a transfer chamber capable of processing a GaAs crystal and transferring it into an ultra-high vacuum envelope. Samples #26 - #30 and #32 (see Table 1) were used to test the transfer chamber for processing and subsequent device transferral.

The initial evaluation yielded disappointing results. However, the GaAs cyrstals used were from a new batch. The problem was resolved in the following way:

Referring to Table 1, Sample #31 was exposed to air after processing, reevacuated and reprocessed. The sensitivity after reprocessing was comparable to the original value. This technique could be used to determine whether the chamber itself or the quality of the GaAs crystals being used at that time was responsible for the poor sensitivities. In addition, the quality of a specific crystal could be determined before it was utilized in a complex device. Following this, Sample #18 was reevacuated and processed in the transfer chamber. A sensitivity comparable to that attained in the demountable belljar was achieved, indicating that the GaAs samples in the new batch were of poor quality. These samples were also observed with the SEM (Scanning Electron Microscope). The results obtained are discussed in more detail under GaAs Crystal Evaluation. The vendor acknowledged the problem and provided one evaluation replacement sample (Sample #34). While this represented an improvement, it did not approach the quality of Batch #2 (see Table 1), which had yielded consistently high sensitivities.

Understanding the limitations presented by the GaAs material, the transfer apparatus was installed in the Transfer Chamber and initial tests made. Since an adequate sensitivity had been achieved on Sample #34, 115 ma/watt at 700 nm (see Table 1), the crystal was reevacuated and used in Transfer #1. Due to a malfunction in the magnetic pick-up component of the internal assembly during transfer the experiment was aborted. Slight modifications were made on the internal transfer assembly and Transfer #2 followed. The sensitivity on this 6.2×10^{18} cm^{-3} zinc-doped reflective-mode crystal just prior to transfer was 84 mA/watt at 700 nm (radiant) and 780 mA/lumen (luminous). The sensitivity of the sealed device was recorded at 67 mA/watt at 700 nm after the cold weld pinch-off separated the final device from the transfer chamber.

Transfer #3 was made reusing Sample #17 (see Table 1) and a post-transfer sensitivity of 100 mA/watt at 700 nm and 911 mA/luman was attained. This device, however, lost all sensitivity overnight. A blue haze was noticed on the envelope wall and was thought to be excess cesium. To test this theory, the crystal surface was desorbed with radiation from a microscope illuminator and the envelope chilled with liquid nitrogen to condense the excess cesium on the envelope walls. Fifty percent of the original sensitivity at 700 nm was recovered. The tube was then allowed to reach room temperature and a steady decrease in sensitivity was observed. By once again desorbing the cesium from the crystal surface and chilling the envelope, 50% of the original sensitivity

was again attained. The desorbtion procedure was then employed on Transfer #2 and 45% of the original sensitivity at 700 nm was recovered. A conclusion was reached that the cesium channel which had been incorporated into the receiver bulb for environmental passivation would be omitted from Transfer #4.

The sensitivity of Transfer #4 just after transfer was recorded at 68 mA/watt at 700 nm. After 40 hours 56% of that sensitivity remained. Cesium desorbtion techniques were again employed, however, this further decreased the sensitivity. In retrospect, having omitted the cesium channel from this device may be the explanation for the behavior of Transfer #4 (i.e., we over-compensated).

Cesium imbalance appeared to be the largest problem in sealed device stability. However, to maintain the program schedule, experiments in this area ceased.

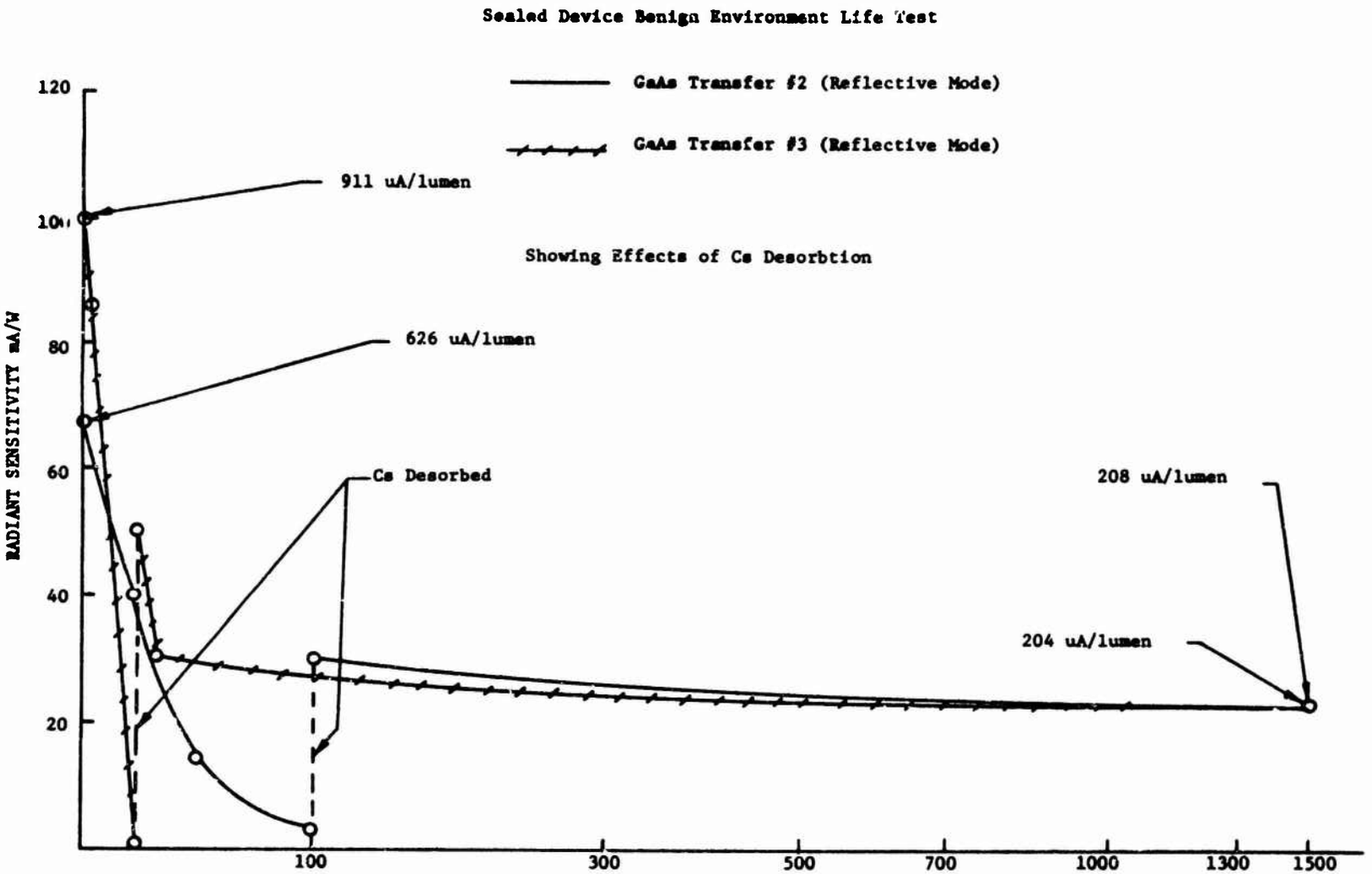

FIGURE 1

LIFETIME STABILITY PLOT

In parallel with the transfer experiments, initial tests were being made on the GaAs self-supporting thin films. Self-supporting thin film #1 was installed in the demountable belljar for reflective mode measurements to ascertain the quality of the material. A detailed evaluation was made and is discussed under GaAs Crystal Evaluation. The reflective mode sensitivities achieved (see Table 1) warranted transmissive mode measurements, and self-supporting thin film #2 was installed in the transfer chamber for these measurements. A surface layer developed on the crystal surface during heat cleaning and no appreciable sensitivity could be attained on this sample. This surface layer was thought to be a result of high temperature reevaporation from the surface of the heater shields during heat cleaning.

The remaining two GaAs thin films received from the vendor were destroyed, forcing the reuse of self-supporting thin film #1. The results are shown in Table 1 and the spectral response in Figure 2. An explanation of these results is given under GaAs Crystal Evaluation.

Finally, Sample #35 was used to explain crystal surface reactions, although widespread dissociation occurred before any results were obtained. Sample #36 was activated to obtain transmissive-mode data on GaAs on GaP crystals, however, a surface layer developed and inhibited any results.

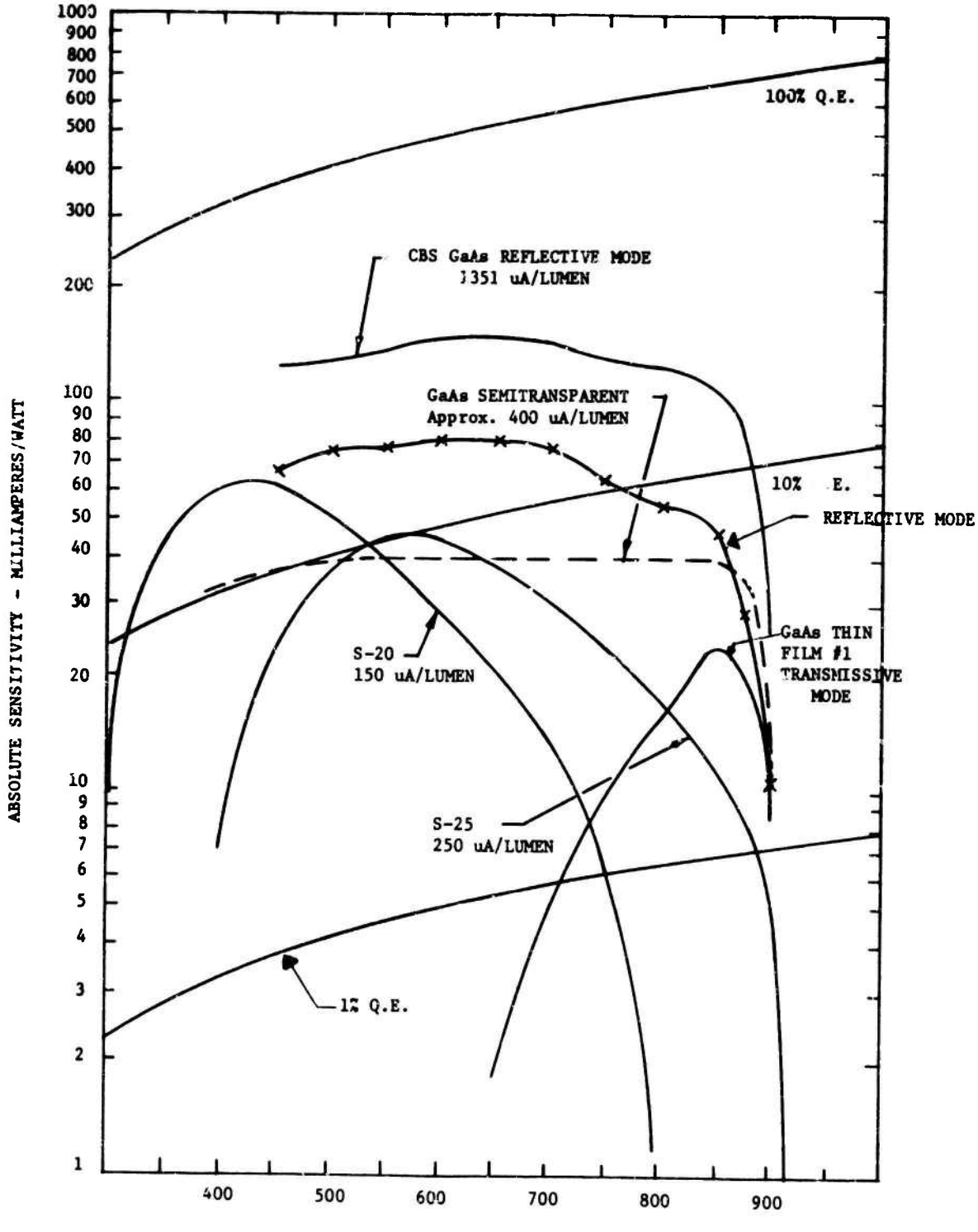

FIGURE 2
SPECTRAL RESPONSE OF GaAs SELF-SUPPORTING THIN FILM #1

SECTION 3

GALLIUM ARSENIDE CRYSTAL EVALUATION

Diffusion length and escape probability are necessary terms in the discussion of III-V photocathodes. For our purpose, diffusion length is the distance that an average, low-energy, photoexcited excess electron will diffuse before recombining. Escape probability is the probability of a photoexcited, low-energy electron in the conduction band escaping into the vacuum.

Diffusion length and escape probability are calculated by solving the yield equation, $Y = P/1 + \frac{1}{\alpha L}$, where Y is the yield or quantum efficiency obtained from the spectral response curve, P is the escape probability, L is the diffusion length, and α is the optical absorption coefficient. Liu[2] derived a simple graphical method of solving the yield equation which will be used here to calculate diffusion length and escape probability.

A short diffusion length indicates poor quality in the GaAs crystal, and is revealed in the long wavelength cutoff region of the spectral response curve. The curve at the lower photon energies softens (i.e., gradually decreases in sensitivity) as opposed to the sharp change in the curve seen in good quality material. This phenomenon is primarily caused by inherent defects in the crystal.

---

2 Yet-zen Liu, Studies of the Cleaning of GaAs Surfaces and of the Photoemission from Bulk GaAs and GaAs Thin Films on Sapphire - PhD Thesis, 1970.

In the course of the evaluation, each crystal was examined prior to and following its complete activation in vacuo. Crystals yielding adequate sensitivities were compared physically and spectrally to those exhibiting poor results. Several groups of materials received from Photoelectronic Materials Corporation were evaluated and compared.

The initial evaluation was done on opaque crystals. Each crystal was a vapor phase <110> epitaxial GaAs layer approximately 10 microns thick on a GaAs support crystal. Four different batches of this material having a doping density of 5-7 x 10^{18} cm^{-3} zinc were received from the vendor. The second batch of material (Batch #2) was the only batch that yielded adequate sensitivities (see Table 1). The physical appearance as observed at 800 X with a conventional microscope exhibited a very low surface defect density. Diffusion length and escape probability calculations were made from the spectral response curve for each of these samples after photoactivation. Diffusion lengths as high as 2.0 microns and escape probabilities reaching .3 were attained from this material.

Material from Batch #1 and replacement crystals (see Table 1) yielded poorer results. The crystals were examined with a scanning electron microscope (SEM) revealing a very high defect density. (see Figure 3). Dislocations propagating through the epitaxial layer from the support crystal were seen, as well as areas of contamination possibly due to etching. Diffusion lengths of less than 1 micron were characteristic of this material.

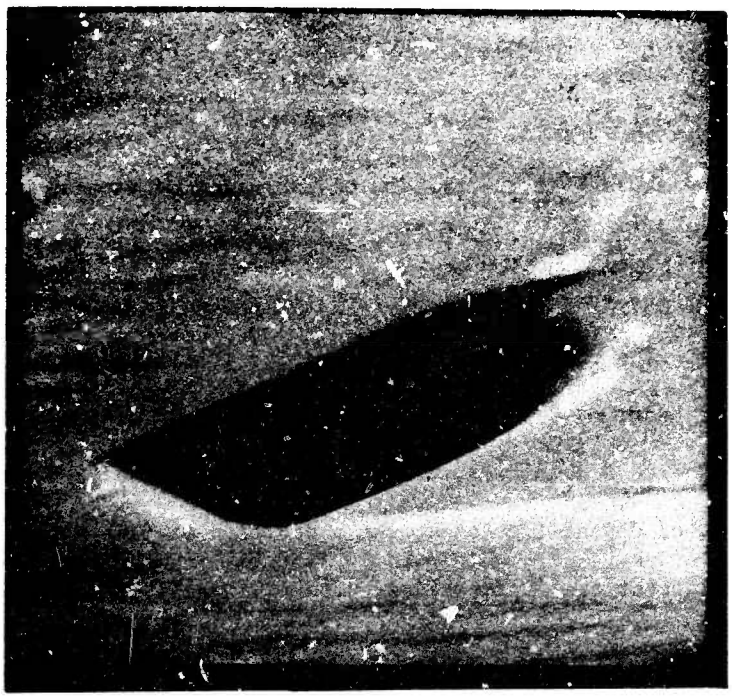

GaAs EPITAXY FAULT (10,000X MAG. SEM)

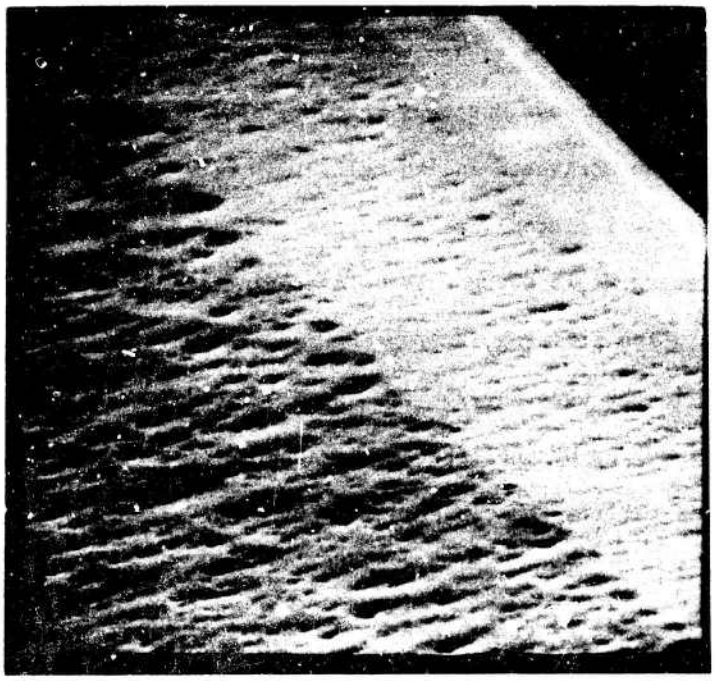

HIGH DENSITY EPITAXIAL DEFECTS (2500X MAG. SEM)

Figure 3 SEM PHOTOGRAPHS OF GaAs EXPITAXY DEFECTS

As discussed in the section on Evolution of Experiments, opaque crystals with doping densities of 1×10^{19} cm^{-3} zinc were activated during the search for the proper doping density for the self-supporting thin film GaAs crystals. The results obtained were also poor, yielding a diffusion length on the order of 0.5 microns. SEM observations of these samples revealed high defect densities, possibly caused by the high doping density. As the amount of dopant increases, the proportion of zinc atoms that enter the lattice interstitially instead of substitutionally also increases, causing gross lattice damage.

The transmissive-mode GaAs on GaP crystals were also evaluated. They consist of a 1 micron thick layer of $6\text{-}8 \times 10^{18}$ cm^{-3} zinc-doped epitaxially-deposited GaAs, on a GaP crystal 75 microns thick. In the transmissive mode the GaP is transparent at photon energies below 2.07 eV. This material displayed poor spectral characteristics at lower photon energies (below 2.07 eV) when activated in the reflective mode (Figure 4). Diffusion lengths of less than 1 micron were calcuated. The "softening of the knee" at these lower energies is thought to be a combination of a short diffusion length and absorption limiting, where a percentage of the lower-energy light is not absorbed in the GaAs layer. The short diffusion length is due to the lattice damage incurred by the lattice mismatch between the GaAs and the GaP. As a result, this material has inherently poor properties for photoemission.[3]

---

3. W. A. Gutierrez, H. L. Wilson and E. M. Yee, Appl. Phys. Lett. Vol. 25, No. 9, 1 Nov. 1974.

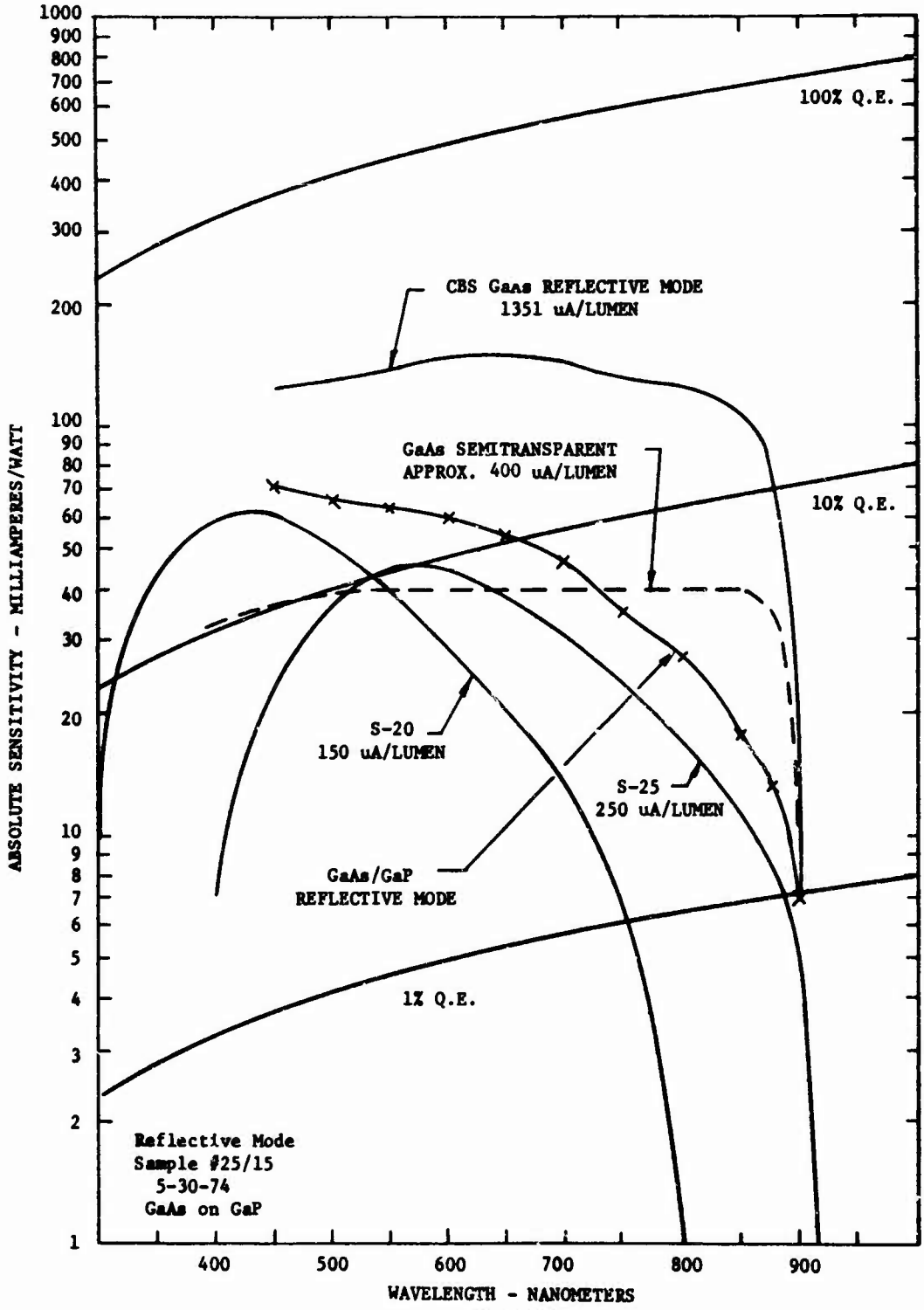

FIGURE 4

SPECTRAL RESPONSE GaAs ON GaP

The self-supporting GaAs thin films were also analyzed. This assembly consisted of an 18 mm diameter GaAs support ring with a 15 mm diameter central active area 1.3 - 1.8 micron thick floated on a ring of indium which in turn was wetted to an evaporated ring of platinum on a 22 mm diameter, 1 mm thick sapphire support window. The crystal orientation was <110> with a doping density of 5-7 x 10^{18} cm^{-3} zinc. The spectral response shown in Figure 2 both in the reflective and transmissive modes, is indicative of a poor diffusion length (in the order of .5 microns). During heat cleaning, great mechanical stress was observed in the thin film in the form of buckling. This pre-stressing is most probably due to the fact that the thin film was grown on GaP, which was etched away prior to setting it on the sapphire window. Again this large lattice mismatch is reflected in the diffusion length.

It is now beneficial to discuss high-energy or X electrons when discussing transmission mode characteristics. The discussion of diffusion length has so far been limited to low-energy or Γ electrons for qualitative analysis of material. X electron diffusion lengths are less than those of the Γ electrons due to the higher probability of recombination. By observing Figure 2 it is seen that a short diffusion legnth is most detrimental in the transmissive mode. The high-energy photoexcited electrons (X electrons) must traverse the entire thickness of the thin film before exiting into vacuum, since the majority of the photons are absorbed within the first few tenths

of a micron of the crystal. Since the diffusion length for the X electrons is less than the thickness of the crystal, little or no response is achieved at these higher energies. In comparison, the X electrons in the reflective mode need only travel the absorption length of the photons, which in this case is less than the diffusion length from an X electron. The Γ electrons are not as greatly affected, since a large percentage are generated deeper in the bulk material and have a longer diffusion length, thus allowing more Γ electrons to escape than X electrons. Absorption data taken on a thin film crystal indicated that the films were in the order of 2 - 2.5 microns thick as opposed to the value of less than 2 microns given by the vendor, which reinforces the above explanation for the limited spectral response. A special note should be made that the results obtained for this material very closely resemble the results obtained by Liu[2] for a 2.5 micron <110> 1×10^{19} cm^{-3} zinc epitaxial GaAs film on sapphire.

It is of particular interest that the optimum photoemissive yield for any of the aforementioned crystals was attained after a surface haze was noticed. This haze was induced by heat cleaning the crystal at the dissociation threshold temperature of GaAs. Samples exhibiting this haze were observed under a conventional microscope at a magnification of approximately 800X. Globules of precipitated gallium resulting from dissociation were physically observable on the surface. These observations were verified by the scanning electron microscope at 3000X. At this magnification, the gallium globules were more evident, with predominance at defect sites such as scratches, epitaxy pits, and crystal dislocations. The role of this surface haze will be discussed later.

SECTION 4

OPTICAL INPUT SYSTEM

4.1 METHOD OF MONITORING PHOTOSENSITIVITY

In order to calculate the emission of photon-excited electrons from the GaAs crystal surface, the characteristics of the radiation incident on the crystal must be known and the emitted electrons must be detected. Also, to minimize surface desorbtion effects during activation, a limit is placed on the maximum current density to be drawn from GaAs emitters. This is accomplished by limiting the total flux input to the GaAs crystal.

Assuming a final sensitivity of 100 mA/W, the spectrally corresponding maximum flux density should not exceed 2.5×10^{-7} W/cm^2. However, in the initial stages of activation when the sensitivity could be < 1 mA/W, this same level of flux will result in a cathode current density of only 2.5×10^{-10} A/cm^2. Detection of such a small current is accomplished by using a 150 Hz chopped optical input to the photocathode and phase-lock detection of the collector current. Excellent noise immunity can be obtained, and the output of the phase locked detector is displayed on a strip chart recorder.

As shown in Figure 5, the chopped optical signal is coupled to the vacuum envelope via a fiber-optic light pipe and an x, y, and z translating f/5 achromatic lens system. Spectral and neutral density filters were placed in the optical path to cover the range 400 to 900 nm in 25 nm increments. The half power bandwidth of the filters was nominally 5 nm, permitting adequate resolution in the skirt regions of the GaAs photoemitter spectral response curve. A mirror system was incorporated within the processing transfer chamber to allow both the reflective and transmissive modes of operation.

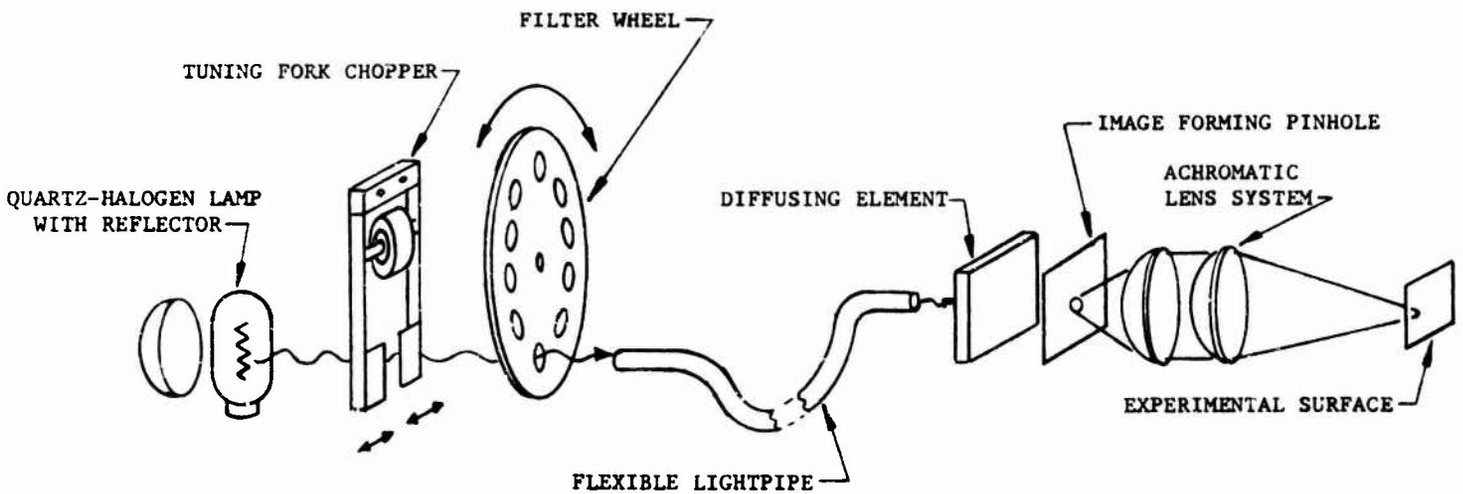

FIGURE 5 OPTICAL INPUT SYSTEM
GaAs PHOTOEMITTER

4.2 CALIBRATION OF PHOTOEMISSION MONITORING EQUIPMENT

The photoemission monitoring equipment was carefully calibrated against NBS-traceable standards as follows:

a) The basic standard used for this purpose was an Optronics Laboratory, Inc. calibrated 200W quartz halogen standard lamp. This served as the source against which both a H.P. Type 8334A/8330A Radiant Fluxmeter and an Eppley 24 Junction Thermopile with Keithley Microvolt meter were standardized.

b) The optical radiation source used for processing and post process evaluation of the GaAs photoemitter was measured with the above thermopiles to establish the absolute irradiance at each spectral point.

c) The sensitivity monitoring system (light chopper, lock-in amplifier, strip-chart recorder) was calibrated in a.c. to d.c. calibration at one spectral point.

d) Spectral characteristics of the interference-type filters were measured with a Zeiss M4QIII Prism Monochromator system (using a Reeder Thermocouple, P.A.R. Beam Chopper and Lock-In Amplifier). This instrument is spectrally calibrated against line spectra sources.

Steps b and c were normally conducted on a daily basis.

SECTION 5

EQUIPMENT

5.1 VACUUM STATION I, DEMOUNTABLE BELLJAR

The purpose of the preliminary experiment was to determine the optimum methods of cleaning and activating the GaAs substrate. To expedite the initial experimental work an existing vacuum chamber was used.

The vacuum processing equipment consisted of a demountable stainless steel work chamber 30 cm long and 15 cm in diameter. This chamber was equipped with a full-diameter end window and suitable pumping ports and feedthroughs. It was pumped by a 140 l/s ion pump following initial evacuation by sorbtion type pumps. Bakeable (all metal) valves were arranged to provide isolation of the rough vacuum and high vacuum functions. The work chamber pressure was monitored with a nude ion gauge located in a side port on the chamber. Following a $300^{o}C$ overnight bake, the vacuum system reached a pressure better than 1×10^{-10} torr. This system is displayed in Figure 6.

The early experiments in this system utilized a cesium generator of the chromate reduction (channel) type. The problems encountered with this cesium source are detailed in the section on Evolution of Experiments. This was replaced with a valveable elemental cesium source. Likewise the original silver tube oxygen leak source was replaced with a revised design. These changes, together with the addition of a Residual Gas Analysis Probe (which was originally unavailable) constituted the significant modifications to the system.

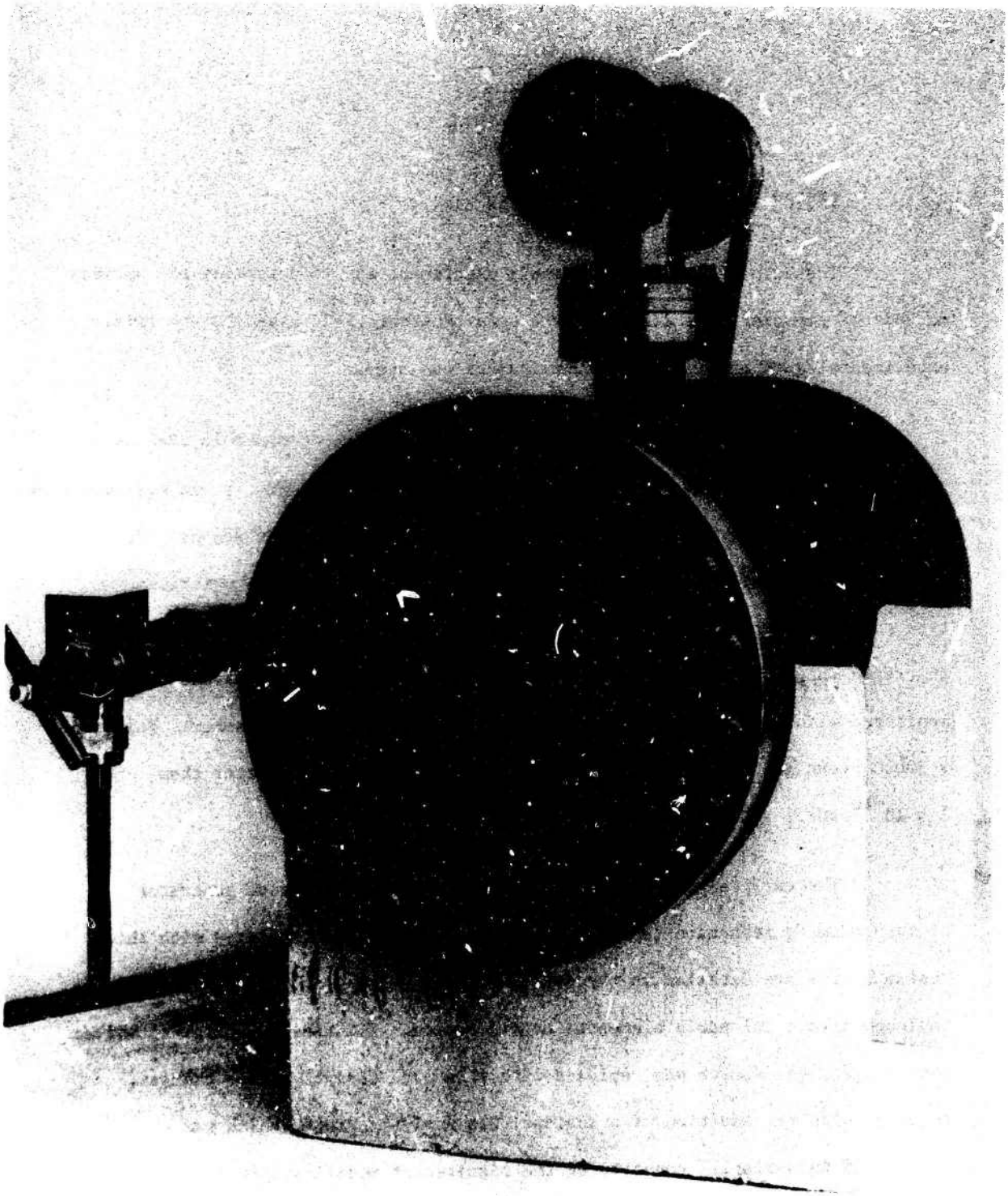

Figure 6 DEMOUNTABLE BELL JAR, VACUUM STATION 1

5.2 VACUUM STATION II, PROCESSING AND TRANSFER CHAMBER

As the program progressed, the experimental plan called for the GaAs crystal substrate to be transferred from the activation chamber into a benign-environment test envelope for further evaluation. An obvious requirement is that vacuum integrity be preserved throughout the operation. A system designed and fabricated to meet these requirements is shown in Figures 7, 8 and 9.

The system consists of an activation chamber incorporating the necessary substrate heater, cesium and oxygen admission devices, and photoemission and temperature monitoring facilities. A magnetic rotary drive moves the crystal substrate holder between the heat treatment and surface activation locations within the chamber. This same rotary drive interfaces with a bellows-type linear motion drive that allows transfer of the activated crystal out of the main chamber and into the test envelope via a copper tubulation. After transferral the copper tubulation is pinched off and the sealed envelope is available for test.

The vacuum system is rough evacuated with N_2-cooled sorbtion pumps. An 80 l/s ion pump connected to the chamber by a 10 cm diameter tubulation permits the chamber to reach a pressure of 1×10^{-10} torr in about 18 hours.

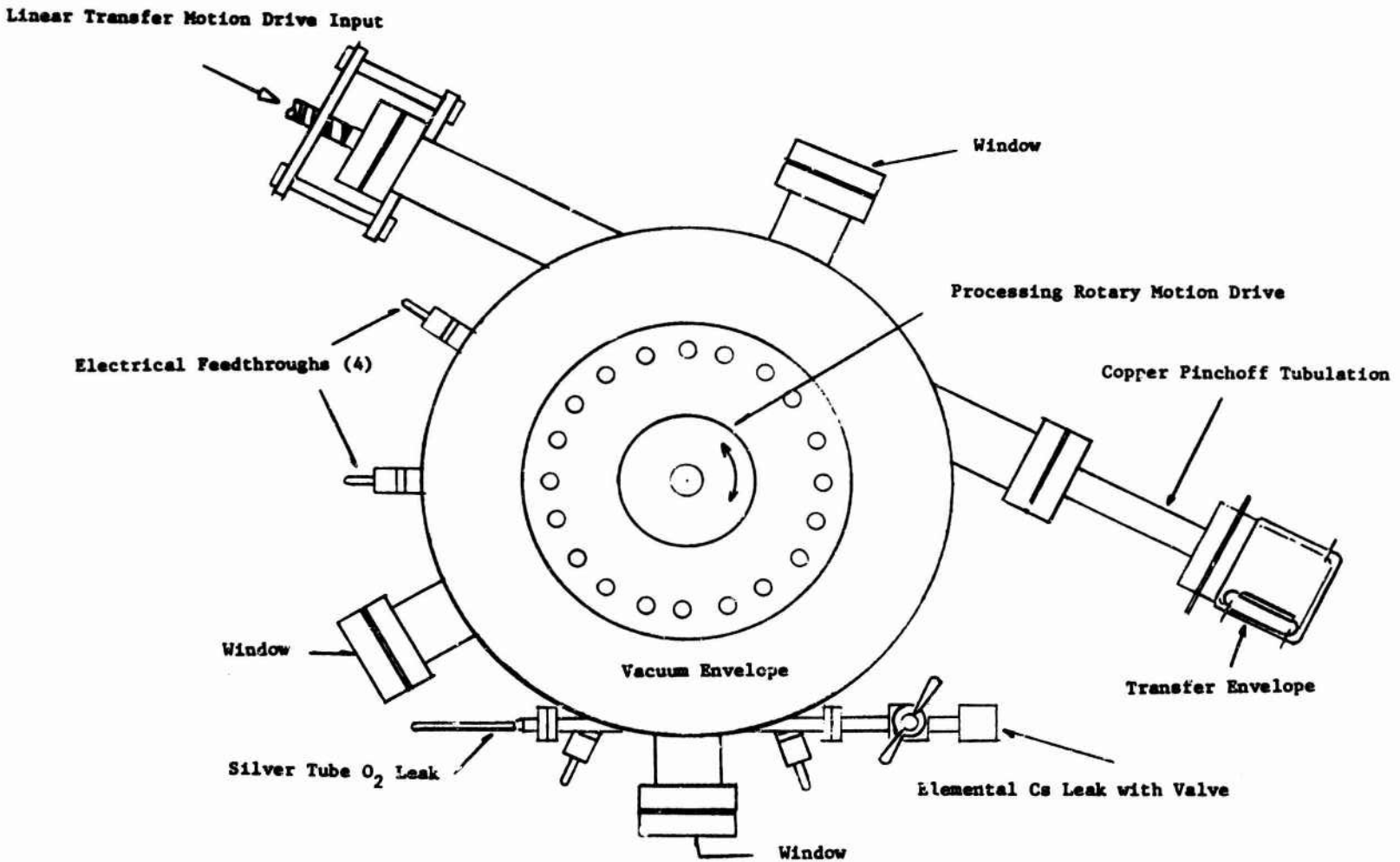

Figure 7 GaAs Photocathode Processing-Transfer Chamber (external arrangement)

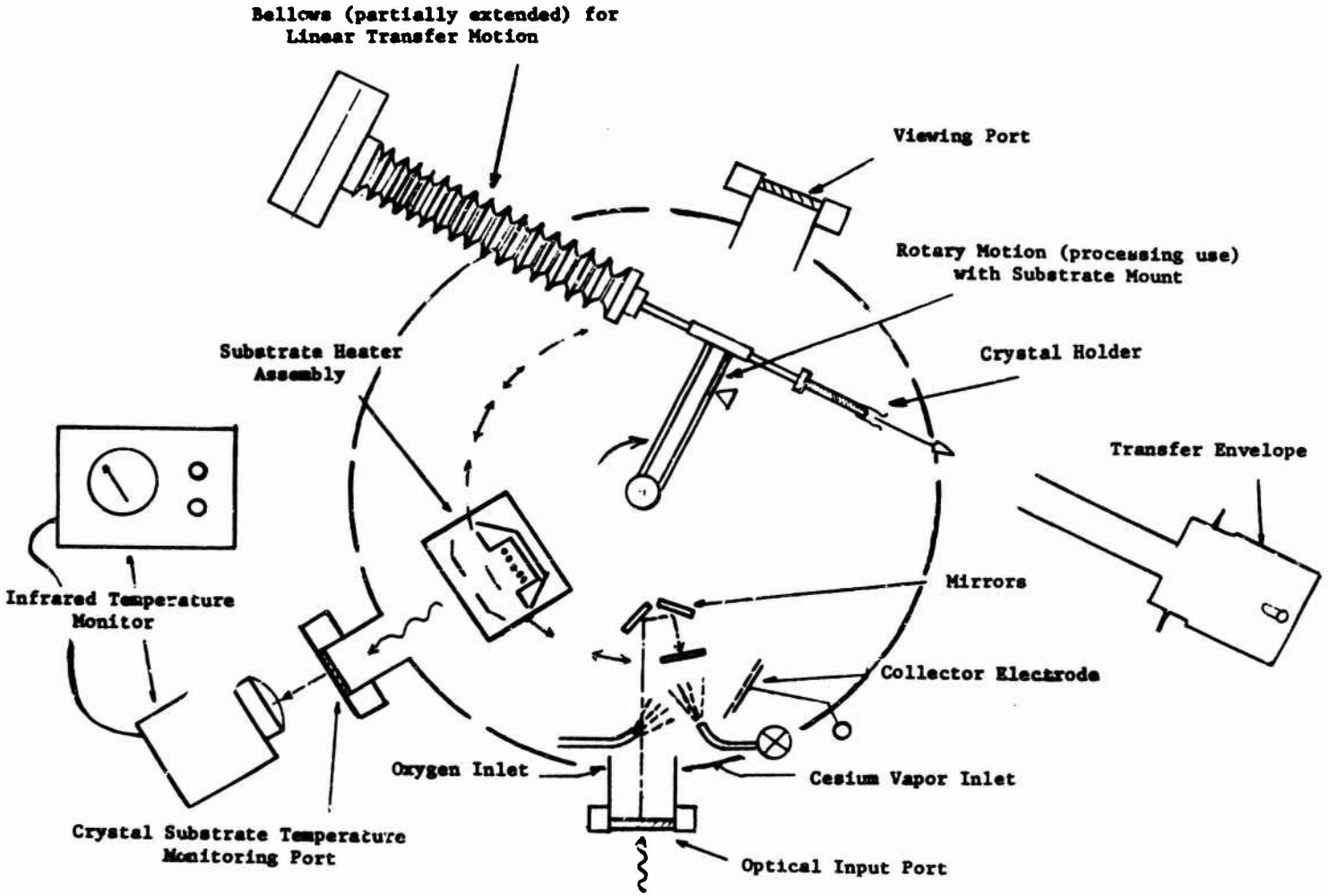

Figure 8 Schematic Layout of Processing & Transfer Components

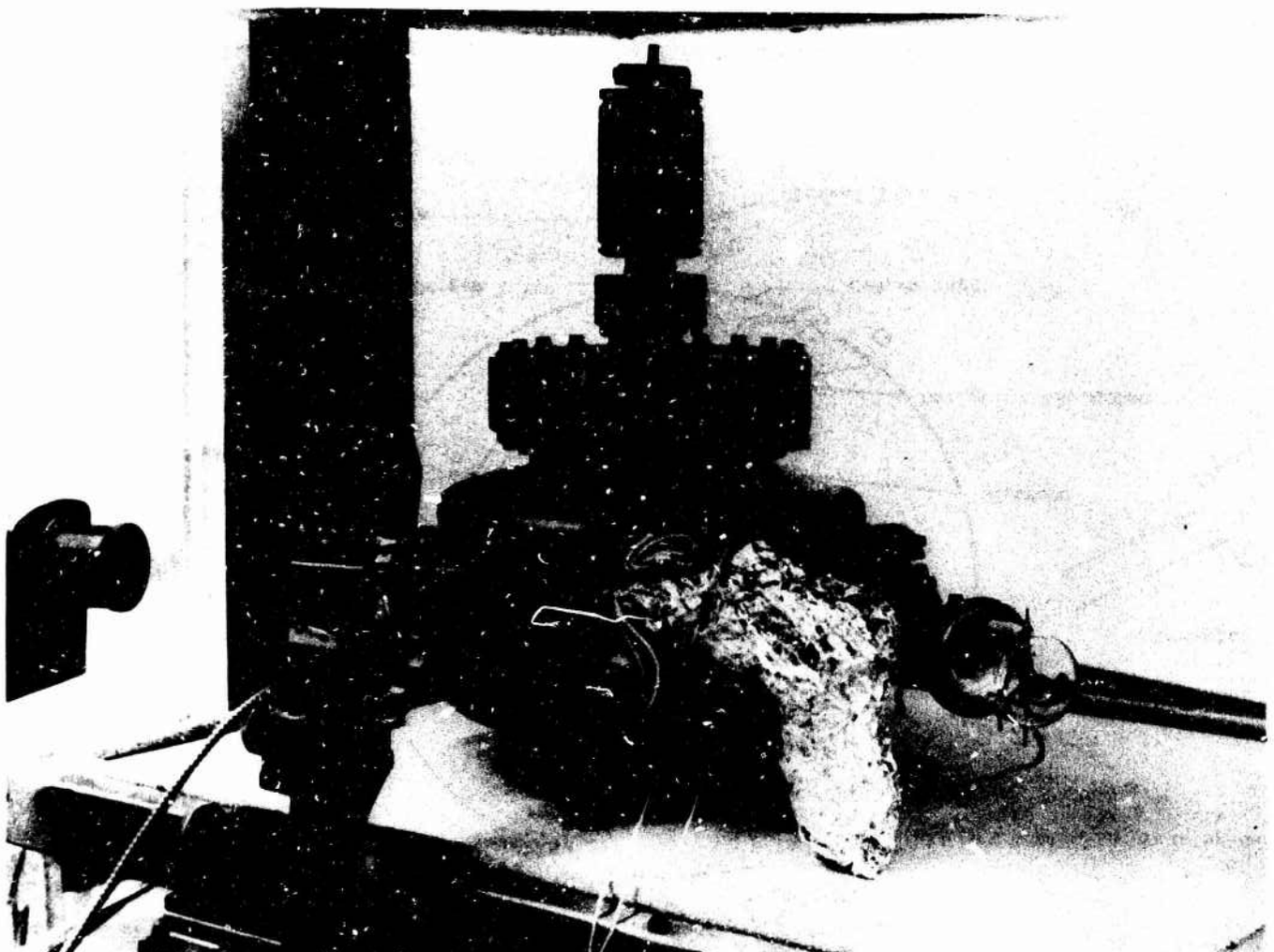

Figure 9 TRANSFER CHAMBER VACUUM STATION II

The process and transfer chamber is fabricated from type 304 stainless steel. It is 25 cm in diameter and 14 cm high, with a volume of 8 liters. All flanges are of the conflat type. The processing system includes a Quadrupole Residual Gas Analysis probe and complete bakeout provisions. The bakeout heaters are interfaced with both temperature and pressure controllers and timers. In normal practice the system pressure is not allowed to rise above 1×10^{-7} torr during bakeout.

The benign environment test envelope consists of a 7056 glass bulb with an internal receiver device to capture the transferred crystal holder. This 5 cm diameter bulb is sealed to a kovar flange which is welded to a mating flange brazed to one end of the copper transfer tubulation. The other end of the transfer tube is connected to the Process Chamber by a conflat flange. The copper tubulation was flattened over its length to permit maximum clearance for the crystal holder in transit. Following transfer the test envelope is isolated by pinching off the copper tube with hydraulic tooling.

5.3 CESIUM CHANNEL SOURCE

Early in the program it was determined that significant ion bombardment of the GaAs substrate was occurring during the cesiation. The ion current could be monitored in the photocathode return connection as a d.c. signal, and ion currents up to 1×10^{-7} A were measured. The heated cesium channel was found to be the source of the ion current. A bias of 90V present between the GaAs substrate and the cesium source provided sufficient ion energy to result in crystal damage. Reorganizing the bias method reduced the ion current and landing energy but did not eliminate the problem completely.

In addition, a major limitation to the SAES cesium channels is the evolution of background gas load during cesium emission. Although an extensive degassing process was followed during system bakeout, a persistant gas load appeared upon cesium generation. However, the reuse of a cesium channel (following system open to air) did result in reduced gas without apparent ill effect to the cesium generation properties. It was not possible to determine the nature of the gas emissions due to the unavailability at that time of a Residual Gas Analyzer.

5.4 ELEMENTAL CESIUM SOURCE

Based on the difficulties encountered with the SAES cesium channels, the decision was made to switch to an elemental type source. Such a source had been developed by Dr. Wolfgang Klein at NVL[1], and this basic design was adopted and modified to interface with the existing equipment as shown in Figure 10. This source consists of a bakeable metal valve mounted on a conflat style flange, and a compression port welded to the other port of the valve. An OHFC copper tubulation which can be pinched off is connected to the compression port. Prior to cesium generation, a glass vial of vacuum-distilled cesium liquid is introduced into the open end of the copper tube which is then pinched off. Following system evacuation with the valve open, the valve is closed and the glass cesium vial in the copper tube is broken by partially pinching the copper.

The entire assembly is heated by tapes to approximately 100°C during cathode activation and the cesium emission is controlled with the valve. A heated quartz tube is used to transfer the vapor from the flange face to the proximity of the GaAs crystal within the belljar. The valve also provides vacuum isolation for the cesium source during substrate changes. One cesium charge will allow many substrate activations.

---

1 Wolfgang Klein, Rev. Sci. Instrum. 42, July 1971.

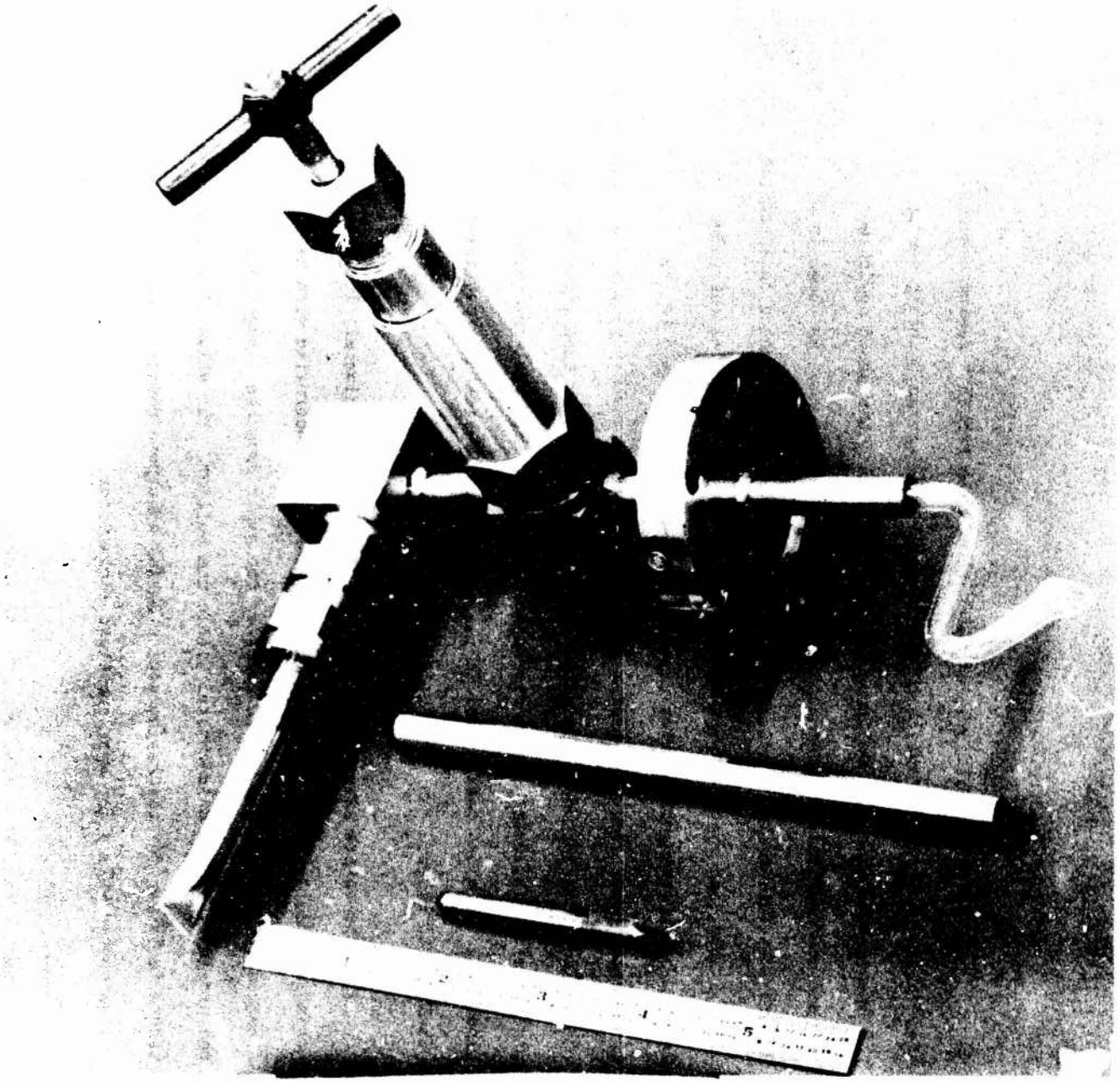

Figure 10 CESIUM ADDMISSION SYSTEM

To improve the efficiency of this source, we incorporated a cesium transport duct in the system. This duct, consisting of a quartz tube, transferred the vapor from the valve output port to the crystal proximity. A perforated tantalum "hat" on the tube end served to diffuse the emitted vapor flow. A simple heater wound on the exterior of the quartz tube aided in the vapor transport and reduced the dribble time (after the cesium valve closure) to a minimum.

5.5 INTERIM CESIUM SOURCE

The components required for the valveable cesium source were long delivery items and an alternate design was fabricated as an interim measure. The source consisted of a sealed glass ampoule containing a small quantity of vacuum-distilled cesium. One end of the ampoule was drawn out to form a capillary tube (also sealed). The ampoule was mounted within the vacuum system with the capillary end directed at the GaAs substrate. A tantalum heater was wrapped around the ampoule to provide a control on cesium vapor generation. Following system bakeout and pumpdown, the capillary end of the ampoule was cracked off mechanically via a rotary motion feedthrough, and the generator was ready for use.

This source was less than successful. In practice, the cesium within the ampoule migrated in an uncontrollable manner following capillary crackoff. It was impossible to activate a GaAs crystal to any significant sensitivity using this source and it was abandoned.

5.6 OXYGEN ADMISSION SYSTEM

During the initial activation experiments, we had used a commercially available silver tube oxygen leak as the source of activating O_2. This device yields oxygen of high purity and the leak rate is easily controlled by varying the silver tube temperature. As supplied, the device has many graded glass to metal seals and a design which is difficult to thoroughly outgas. In operation we were plagued with numerous minor leaks due to the graded seals. The device was redesigned to a completely reliable, smaller, all-metal design mounted directly on a conflat flange that can be completely outgassed during system bakeout. In operation, oxygen pressures between the system base pressure and 1×10^{-6} torr can now be easily generated and controlled.

5.7 CRYSTAL HOLDER

A multifunction crystal holder supports the GaAs substrate during the "in vacuo" activations, and in the test envelope after transfer. The outer frame of the holder mates with both the processing equipment and the magnetic pickup for final transfer. A similar holder was used for demountable belljar experiments. The crystal holder suspends the GaAs crystal by means of crimped fine tantalum wires, limiting the thermal sink effects of the support structure.

The freely-suspended crystal was directly heated by means of a pancake-form tantalum heater located 2.5 cm (1.5 cm in the demountable belljar) behind the substrate. The substrate temperature was monitored with an Infrared Radiation Pyrometer (IRP) which views the substrate (through the vacuum envelope window) at an oblique angle. This viewing angle is such that the direct radiation from the heater cannot be seen "through" the GaAs crystal. To calibrate the IRP, we utilized a low mass thermocouple which is in contact with the front face of the crystal substrate. After allowing the substrate-thermocouple combination to reach a stable temperature (typically 3-4 mins. to stabilize at 600°C), we could relate the IRP indication to the thermocouple measurement. In practice we relied on the reproducibility of the IRP, which responds rapidly to the crystal temperature changes. A further calibration point for the temperature monitoring system was obtained by raising the temperature to the crystal disassociation temperature. No thermocouple was incorporated in the holders after these calibrations.

The thermal inertia of the complete crystal holder assembly is such that a crystal temperature above 600°C can be attained in approximately 10 sec. with recovery to less than 60°C within 1 minute following heater shutdown. This was important to prevent ambient recondensation upon the crystal.

In the demountable belljar the holder was suitably insulated to allow bias potentials to be applied during photosensor activation. However, for transfer chamber application the holder is at ground potential.

5.8 RESIDUAL GAS ANALYSIS

Throughout most of the GaAs Photosensor Development Program a Residual Gas Analyzer (RGA) was connected to the vacuum equipment. This was a Granville-Phillips Spectrascan 750 Quadrupole System[1]. The system gas environment was studied with this instrument from start of bakeout through surface activation. In general, the indications from the RGA confirmed that the system was clean and leak free, however two trends were detected with the equipment:

a. An occasional excessive water vapor signature was detected following a "normal" bakeout cycle that would not show up on the Ionization Gauge reading. Although the source of this excess could not be determined, it could be eliminated by additional bakeout.

b. During the first hours of operation of the valveable cesium source, a marked hydrogen background was seen. It was traced to the copper tubulation containing the cesium ampoule. Although continued operation of the cesium source reduced the hydrogen evolution considerably it was never completely eliminated. Changing the cesium ampoule (and copper tubulation) restored the high hydrogen background.

It is significant to note that even with a clean background indication from the RGA, the GaAs activation process would not yield good results unless the system was first passivated (by cesium admission, etc.)

---

1 Manufactured by Finnegan Instrument Corp.

SECTION 6

AN EXPLANATION OF THE REVISED UNDERSTANDING OF THE ROLE OF CESIUM IN THE GaAs PHOTOEMISSION PROCESS

The experimental results accumulated during this program indicate that the photocathode activation of the GaAs crystal is significantly more complex than the widely accepted model. Based on our experimental findings it is our hypothesis that the role played by cesium atoms in the activation process is not limited to a surface effect. There are strong indications that a bulk crystal effect is present and this can result in significantly improved emission characteristics. The data accumulated during the experimental program indicates the following:

1. Optimum sensitivity is not obtained until a surface haze is seen on the GaAs crystal. This haze indicates surface saturation with (and agglomeration of) gallium.

2. A good emitting crystal yields optimum emission after the low temperature part of the high-low temperature cleaning and processing cycle[4]

3. As processing continues through the steps of heat cleaning and Cs-O admission (cycles), the activation requires an increasing quantity (total charge) of Cs. In addition, the emission level seen on only the first Cs peak (prior to O_2 admission) on each cycle increases for the initial cycle and then decreases until a stable level is reached.

---

4. D. G. Fisher and G. O. Fowler, Conf. on Photoelectric and Secondary Electron Emission 1973 Univ. of Minn.

4. The optimum sensitivity is not achieved until some number of cycles are performed.

5. Lumping the total heat treat times in one long exposure does not yield sensitivities approaching optimum.

6. The number of heat treatments is more important than the length of the heat treatment.

7. The temperature for the low cycle is most critical.

8a. A crystal that has been activated to near optimum sensitivity and then exposed to the atmosphere can be reactivaced to a similar sensitivity.

8b. The reactivation takes fewer cycles than did the original activation.

9. Area uniformity and time stability of emission improves as optimum sensitivity is approached.

The explanation for these effects is given in the succeeding paragraphs.

The band diagram for the GaAs crystal after its initial heat cleaning is shown in Figure 11. A uniform heavy doping density is assumed through the bulk to the surface designated as the P+ region (we are ignoring the existence of n-type surface states at this point).

Figure 12a represents the GaAs crystal during activation after an initial charge of cesium is admitted. Referring to the diagram, D is the drift length or field-assisted region where the photoexcited electron is under the influence of an internal field. Here the band bending is governed by the bulk crystal doping. The electron affinity (E_A) is the energy difference between the bottom of the conduction band in the bulk and the vacuum level, and at this stage of the activation process is positive, since the vacuum level is above the bottom of the conduction band. E_{AO} is the energy difference between the vacuum level and the bottom edge of the conduction band at the crystal-cesium interface.

With the addition of oxygen and more cesium, which forms a dipole layer, the surface work function (ϕ), which is the energy difference between the vacuum level and the Fermi level, is lowered to a point of negative electron affinity (NEA) [5] and is shown in Figure 12b.

In Figure 13 the GaAs crystal is represented just after heat cleaning and some cycles later than Figure 12. At this point a surface haze is observed which is due to the release of arsenic during heat cleaning, leaving a precipitation and subsequent agglomeration of gallium on the surface.

---

5. Ronald L. Bell, William E. Spicer, Proc IEEE Vol 58, 11, Nov. 1970.

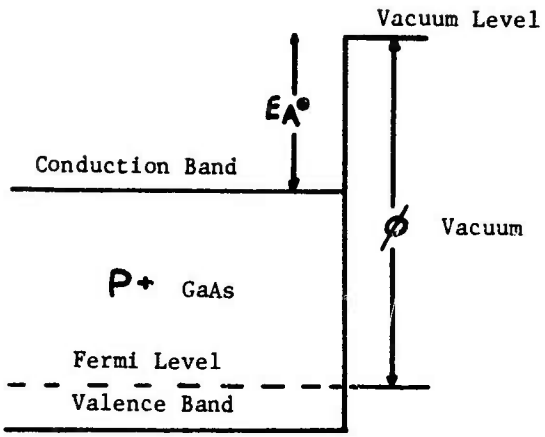

Figure 11 HEAT CLEANED P^+ GaAs

FIGURE 12a

GaAs with Addition of Cesium only

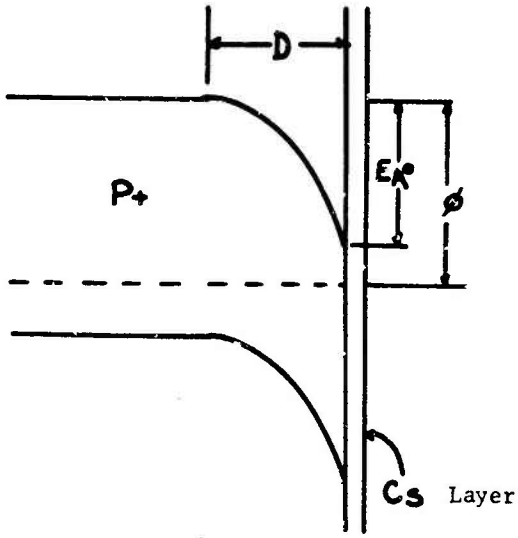

FIGURE 12b

Cs_2O Dipole Formation on GaAs

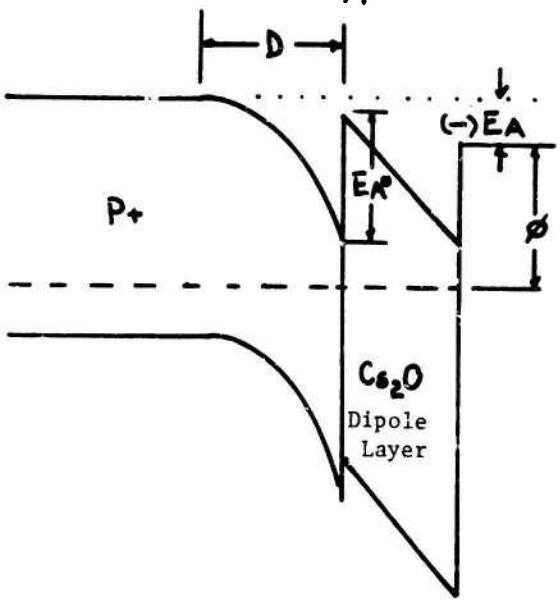

Figure 12 GaAs CRYSTAL

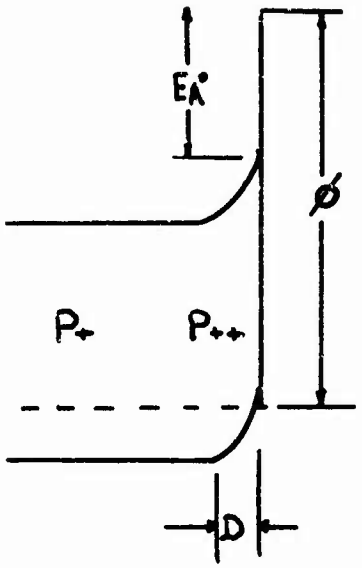

FIGURE 13
Heterojunction Formation

This raises the effective surface doping density to P^{++} forming a hetero-junction which is shown in the band diagram.

Figure 14a represents the crystal after some cesium has been added to the P^{++} surface, compensating it initially to an intrinsic level with additional cesium needed to complete the pinning of the bands (Figure 14b). It should be noted here that E_A is larger than that of Figure 12a and D is less because of the higher effective surface doping density. With the addition of the dipole layer (oxygen and more cesium), ϕ approximates neutral electron affinity where the bottom of the conduction band in the bulk is at the same energy as the vacuum level (Figure 14c). This represents an overall increase in escape probability when compared to Figure 12b due to a favorable tradeoff between D and ϕ. As a result there is an increase in quantum efficiency.

In summary, there is a strong indication that the GaAs crystal is significantly modified by the combination of heating and activation cycles.

It is our opinion that a hetero-junction is formed at the crystal surface by a combination of out-diffusion of As and interaction of surface-bound Cs with the critically-heated crystal lattice. The resultant hetero-junction will reduce the depth of the band bending region. However, a higher density of surface states would be required to pin this more highly doped surface. The requirement for an increase in Cs charge as the surface haze appears supports this contention.

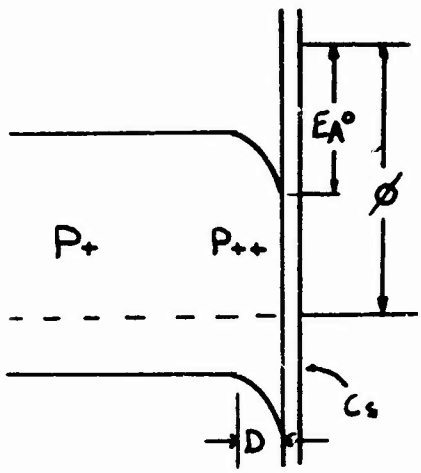

FIGURE 14a

GaAs during Cesiation Compensating
Surface to an Intrinsic Level

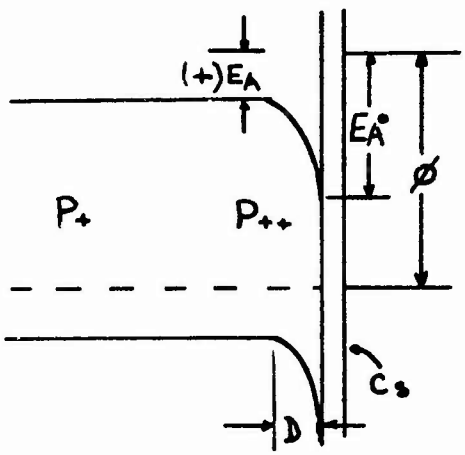

FIGURE 14b

GaAs after Completing
Cesiation only

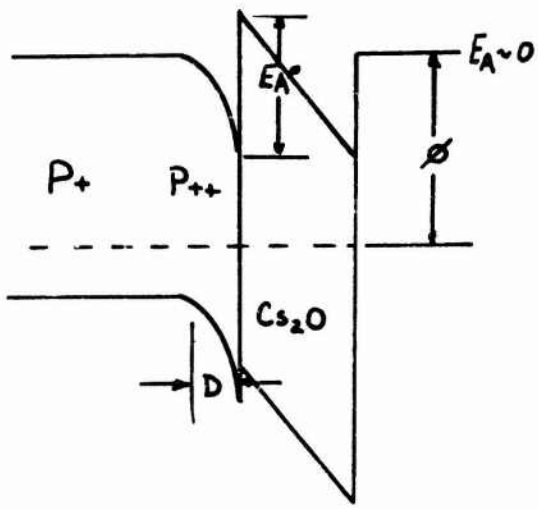

FIGURE 14c

Dipole Formation on Heterojunction

Figure 14 ENERGY DIAGRAMS

The finding that summing the heating times in one exposure does not yield successful results, leads one to believe that the role of the thermal cycles is not limited to impurity desorbtion, but continues on to provide the interaction between the Cs and the GaAs crystal. It is not understood whether the Cs remains interstitally bound or outdiffuses, leaving a disrupted lattice. The contention that a heterojunction is formed by irreversable crystal changes is supported in part by the ease by which sensitivity is regained in a crystal that has been exposed to atmosphere.

SECTION 7

CONFERENCES DURING THE PROGRAM

On July 19th, 1973, Terence Roach visited the facilities of the Photoelectric Materials Corporation (PMC) in Alexandria, Virginia. PMC was the vendor supplying the GaAs crystals, and this meeting was to coordinate our activities.

Dr. Samuel Ward and Terence Roach visited the Night Vision Lab at Ft. Belvoir, Virginia, on January 23, 1974. They discussed III-V photocathode technology with Fred Carlson.

On January 24, Dr. Ward and Mr. Roach visited the new facilities of PMC. In addition to surveying the operation, an extensive engineering conference was held with Dr. Dieter Pommerrenig of PMC, with reference to both self-supporting GaAs crystals and materials for 1.06 μ operation.

Mr. Roach travelled to PMC again on September 29, 1974, to discuss problems with some PMC-supplied GaAs crystals.

SECTION 8

CONCLUSIONS

An activation process has been developed that can yield consistent reflective mode sensitivities greater than 125 mA/W at 700 nm and 1100 μA/lumen. We have developed a firm understanding of the activation physics which leads us to hypothesize the existence of a heterojunction at the emission surface of an activated GaAs crystal. A system of processing and transfer equipment has been designed and fabricated to meet the program requirements. This equipment has performed reliably.

During the experimental work we discovered that an activated GaAs crystal can be reactivated after exposure to atmosphere.

Two problem areas have been identified. The photocathode stability was unacceptable when transferred into the test envelopes. This appears to be a function of envelope environmental conditioning. A more significant problem is the basic GaAs crystal quality. The probability of fabricating a GaAs photocathode having good sensitivity and uniformity is basically dependent on the crystal properties. Our vendor-supplied crystals were of generally inadequate quality. Only one batch of crystals gave consistently good results.

SECTION 9

RECOMMENDATIONS FOR FURTHER DEVELOPMENT

Our findings during the current development program indicate other experimental areas that should receive consideration for continued work:

a. Develop a viable technique of conditioning and monitoring the device test envelope prior to transferring the activated GaAs crystal. The successful accomplishment of this conditioning passivation is absolutely necessary if a useful cathode life within a camera device is to be achieved.

b. Collect and evaluate a complete data package on life performance of transferred GaAs cathodes.

c. Compatibility testing of GaAs photocathode with actual camera components.

d. Develop in-house crystals.

The eventual goal of an extended program such as this would be the provision of a photocathode for integration in a recycled camera. It would offer the following performance improvements compared to the present S-20 photocathode:

	S-20	GaAs
Visible Response (luminous sensitivity)	150 μA/lumen	> 300 μA/lumen
6943 Å Response	≈ 15 mA/W	> 36 mA/W
6943 Å Quantum Efficiency	≈ 2.5%	~ 6%

A further advantage is gained from the reprocessing capability of a GaAs substrate. This allows selection for optimum crystal properties prior to installation in the camera, and recycling of a camera with minimal photocathode costs.

MISSION
of
Rome Air Development Center

RADC is the principal AFSC organization charged with planning and executing the USAF exploratory and advanced development programs for information sciences, intelligence, command, control and communications technology, products and services oriented to the needs of the USAF. Primary RADC mission areas are communications, electromagnetic guidance and control, surveillance of ground and aerospace objects, intelligence data collection and handling, information system technology, and electronic reliability, maintainability and compatibility. RADC has mission responsibility as assigned by AFSC for demonstration and acquisition of selected subsystems and systems in the intelligence, mapping, charting, command, control and communications areas.